Importance of Basic Residues and Quaternary Structure in the Function of MIP-1β: CCR5 Binding and Cell Surface Sugar Interactions†

Jennifer S. Laurence,‡,§ Cédric Blanpain,|| Anne De Leener,|| Marc Parmentier,|| and Patricia J. LiWang*,‡

Department of Biochemistry and Biophysics, Texas A&M University, TAMU 2128, College Station, Texas 77843-2128, and IRIBHN, Université Libre de Bruxelles, Campus Erasme, 808 route de Lennik, B-1070 Bruxelles, Belgium

Received November 9, 2000; Revised Manuscript Received February 9, 2001

ABSTRACT: Chemokines direct immune cells toward sites of infection by establishing a gradient across the extracellular matrix of the tissue. This gradient is thought to be stabilized by ligation of chemokines to sulfated polysaccharides known as glycosaminoglycans (GAGs) that are found on the surface of endothelial and other cells as well as in the tissue matrix. GAGs interact with chemokines and in some cases cause them to aggregate. The interaction between cell surface GAGs and chemokines has also been postulated to play a role in the anti-HIV activity of some chemokines, including MIP-1β. Since many proteins interact with GAGs by utilizing basic residues, we mutated R18, K45, R46, and K48 in MIP-1β to investigate the role of these residues in GAG binding and CCR5 function. We find that no single amino acid substitution alone has a dramatic effect on heparin binding, although change at R46 has a moderate effect. However, binding to heparin is completely abrogated in a mutant (K45A/R46A/K48A) in which the entire "40's loop" has been neutralized. A functional study of these mutants reveals that the charged residues in this 40's loop, particularly K48 and R46, are critical mediators of MIP-1β binding to its receptor CCR5. However, despite the partially overlapping function of the residues in the 40's loop in binding to both CCR5 and heparin, the presence of cell surface sugars does not appear to be necessary for the ability of MIP-1β to function on its receptor CCR5, as enzymatic removal of GAGs from cells results in little effect on MIP-1β activity. Because the means by which the chemokine gradient transmits information to the recruited cells is not well defined, we also mutated the basic residues in MIP(9), a truncated form of MIP-1β that is impaired in its ability to dimerize, to probe whether the quaternary structure of this chemokine influences its ability to bind heparin. None of the truncated variants bound as well as the full-length proteins containing the same mutation, suggesting that the MIP-1β dimer participates in heparin binding.

Chemokines are small proinflammatory proteins released by cells as the result of insult and infection. These chemoattractive molecules recruit leukocytes by establishing a gradient, which directs immune cells toward infected tissue. Despite the well-confirmed immunological evidence for this phenomenon, little detailed information directly describing how the chemokine gradients are formed has been reported. Chemokines bind to seven transmembrane G-protein-coupled receptors to initiate transduction and have also been shown to bind to glycosaminoglycans (GAGs),[1] a group of modified polysaccharides that line the extracellular surface of endothelial cells. It has been postulated that chemokines may bind to these GAGs to form an immobilized gradient that would effectively direct leukocytes to the appropriate tissue (*1*). GAGs are known to interact with many secreted proteins and can deliver these proteins to their receptors. GAGs have been shown to enhance the affinity of fibroblast growth factor (FGF) for its receptor (*2*) and to facilitate dimerization of the receptor, which is required for signal transduction (*3*). Due to the presence of the negatively charged sulfate moieties on the GAGs, proteins tend to utilize basic residues as a means of binding these sugars, as has been confirmed by the structures of basic and acidic fibroblast growth factors in complex with heparan sulfate (*4*−*6*). The sulfated GAGs heparin, heparan sulfate, and chondroitin sulfate have been shown to interact with chemokines (*7*−*9*). Although no structure is available for a chemokine−GAG complex, mutational analysis has demonstrated the necessity of

† Funding was provided by the National Science Foundation (Grant MCB 9733907) and by the American Heart Association (Grant 0050798Y). M.P. was supported by the Actions de Recherche Concertées of the Communauté Française de Belgique, the French Agence Nationale de Recherche sur le SIDA, and the BIOMED and BIOTECH programs of the European Community (Grants BIO4-CT98-0543 and BMH4-CT98-2343). C.B. is Aspirant of the Belgian Fonds National de la Recherche Scientifique.

* To whom correspondence should be addressed: Department of Biochemistry and Biophysics, Texas A&M University, TAMU 2128, College Station, TX 77840-2128. E-mail: pliwang@tamu.edu. Telephone: (979) 845-5616. Fax: (979) 845-9274.

‡ Texas A&M University.

§ Current address: Department of Biological Sciences, Purdue University, 1392 Lilly Hall, West Lafayette, IN 47907-1392.

|| Université Libre de Bruxelles.

[1] Abbreviations: CCK, cholecytokinin; CCR, CC chemokine receptor; CHO, Chinese hamster ovary; DSS, 4,4-dimethyl-4-silapentane-1-sulfonate; DMEM, Dulbecco's Modified Eagle's Medium; GAG, glycosaminoglycan; HIV, human immunodeficiency virus; HSQC, heteronuclear single-quantum coherence; MALDI-MS, matrix-assisted laser desorption mass spectrometry; FACS, fluorescence-activated cell sorting; BSA, bovine serum albumin; MCP-1, monocyte chemotactic protein 1; MIP-1, macrophage inflammatory protein 1; NMR, nuclear magnetic resonance; PF-4, platelet factor 4; RANTES, regulated upon activation, normal T cells expressed and secreted; TFA, trifluoroacetic acid; WT, wild-type.

10.1021/bi002593w CCC: $20.00 © 2001 American Chemical Society
Published on Web 03/24/2001

charge−charge interactions in this association (*8*, *10*−*13*).

Members of the chemokine family of proteins share a conserved fold composed of three antiparallel β-strands and a C-terminal α-helix. Subfamilies are denoted by the positioning of conserved cysteines at the N-terminus of the protein, with the two major subfamilies either having two contiguous cysteines (the CC subfamily) or containing an extra amino acid between these cysteines (the CXC subfamily). Functional analysis of several chemokines has led to the general conclusion that the N-terminal portion of the protein preceding the Cys motif is responsible for signaling (*14*−*19*), while the N-loop region (residues 13−20) promotes tight binding to the chemokine receptor (*17*). While some chemokines are monomers even at high concentrations (*20*−*23*), others are dimers with dissociation constants ranging from 500 nM (*24*) to 50 μM (*25*). In addition, several chemokines (including MIP-1β, MIP-1α, and RANTES) have the tendency to self-associate further, forming larger multimeric complexes in a pH-dependent manner. The two major chemokine subfamilies each exhibit a distinct dimer form. The CXC interface is formed by interactions between the β1 strands of the two subunits, whereas the CC type associate along their N-termini (*26*−*31*). While the chemokine monomer appears to be sufficient for receptor binding and to activate calcium release (*19*, *24*, *32*), GAGs have been shown to promote chemokine aggregation (*7*) and may cause the quaternary structure of the protein to differ from that observed in structural studies.

Several conserved basic residues exist within each chemokine subfamily. CXC chemokines tend to have basic residues in their C-terminal helix that appear to participate in GAG complex formation (*8*), whereas the CC class contains clusters of positively charged residues in two loops. The CC chemokine MIP-1β contains six positively charged residues, exclusively located in two potential heparin-binding loops. Residues R18, K19, and R22 immediately follow the receptor binding "N-loop" region, in such a way that these two segments form a single continuous loop from the CC motif to the first β-strand. K45, R46, and K48 are located between β2 and β3 and are positioned on the same face of the protein as the N-loop region. Despite the conserved patterns of basic residues, there is some disparity in the use of these residues for GAG binding. Mutational analysis of MIP-1α and MIP-1β has shown that several basic residues participate in GAG binding (*10*−*12*). While the sequences of MIP-1α and MIP-1β are 67% identical, it appears that the extent to which these proteins rely on specific basic residues varies. The most prominent reported difference between MIP-1β and MIP-1α is the importance of Lys48, which when changed to Ala in MIP-1α results in a complete lack of heparin binding; the analogous mutation in MIP-1β has no effect on the protein's affinity for heparin (*10*, *11*).

The CC chemokines MIP-1α, MIP-1β, and RANTES are able to block cellular entry of HIV by competing with the virus for receptor binding (*33*−*36*), and both RANTES and MIP-1β were shown to be less effective at protecting cells from HIV infection after the cell surface GAGs had been removed (*37*). Additionally, although it has been suggested that in the presence of soluble GAGs, RANTES acts as a more potent anti-HIV agent (which might suggest a chemokine−GAG complex as the receptor-bound species) (*38*), other studies show that soluble GAGs compete with receptors for binding to MIP-1α (*9*, *39*). In support of a model in which cell surface GAGs are able to sequester chemokines but are not directly involved in the chemokine−receptor interaction, recent studies using genetically modified CHO cells (transfected with CCR5) that are incapable of producing most GAGs showed an unchanged ability of MIP-1β and RANTES to bind CCR5 (*39*). However, MIP-1α bound significantly worse to these cells (*39*).

To delineate specific interactions involved in MIP-1β binding to GAGs, to study the effect of self-association on these interactions, and to determine the effect of these interactions on the overall function of this chemokine, we mutated several of the basic residues in MIP-1β and several other variants, including the monomeric analogue MIP(9). These mutants were tested for their ability to bind CCR5 and to promote intracellular calcium release. In addition, wild-type MIP-1β was tested for its ability to activate CCR5 in the absence of cell surface GAGs and upon addition of soluble GAGs.

EXPERIMENTAL PROCEDURES

Protein Production

MIP-1β and MIP-1β-P8A analogues were expressed from the pET-32/Xa LIC vector (Novagen) and MIP(9) variants from a modified pET vector as previously described (*19*). MIP(9) is a truncated form of MIP-1β that begins with residue Thr9. Proteolysis of the fusion partner with factor Xa was carried out in 20 mM sodium phosphate (pH 8.0). As MIP-1β tends to be aggregated under these conditions, in some cases protease cleavage was observed to proceed more quickly in the presence of 10 nM single-stranded oligonucleotide. Proteins were analyzed by MALDI-MS or amino acid composition to determine whether the correct results were achieved after proteolytic digestion. Nuclear magnetic resonance (NMR) spectra were recorded for each protein to confirm structural integrity. Three MIP(9) variants [MIP(9)-R18A, MIP(9)-K45A, and MIP(9)-K48A] underwent an additional round of refolding when their HSQC spectra revealed the presence of some unfolded protein (as evidenced by intense peaks around a proton chemical shift of 8.3 ppm). The extra refolding step improved the spectra for each of these mutants, after which the proteins were considered folded. MIP(9)-R22A appeared to be mostly unfolded even after two additional attempts to refold this mutant, so it was not studied further.

NMR Data Collection

The data for the MIP(9) variants were collected at 25 °C on a Varian Inova 500 MHz spectrometer equipped with an xyz gradient penta probe. A spectral width of 6000 Hz was used in the ^{1}H dimension and 1600 Hz in the ^{15}N dimension during the HSQC experiments. Spectra for all full-length MIP-1β and MIP-1β-P8A analogues were acquired using a Varian Unity Plus 600 MHz spectrometer equipped with a z-shielded gradient triple-resonance probe. On this instrument, the spectral width was set to 8000 Hz in the ^{1}H dimension and 1600 Hz in the ^{15}N dimension. HSQC spectra were collected with 512* points in the proton dimension and 128* points in the nitrogen dimension. Referencing is relative to DSS, using the method proposed by Wishart et al.(*40*). Data were processed using the program nmrPipe (*41*).

Heparin Chromatography

NMR samples were desalted by being passed over a C8 Sep-Pak column (Waters Corp., Milford, MA) in preparing for heparin chromatography. Samples were injected with a syringe onto the Sep-Pak column, rinsed with approximately 8 mL of a water/TFA solution containing 5% acetonitrile, and eluted in 2−3 mL of a 90% acetonitrile/TFA solution. Samples were dried on a Speed-Vac apparatus and reconstituted in sterile water. Protein concentrations were determined from the absorbance at 280 nm.

Approximately 30 μg of lyophilized protein was taken up in 0.5 mL of 50 mM Tris (pH 7.4) and injected onto a 1 mL Hi-Trap heparin column (Pharmacia, Piscataway, NJ) using a Pharmacia Gradi-Frac system. The column was rinsed with 5 mL of the same buffer followed by a gradient of 0 to 1.0 M NaCl in 50 mM Tris (pH 7.4) at a rate of 0.5 mL/min for 60 min. Buffers were degassed for 5 min prior to each run to minimize the formation of bubbles during the gradient, and the elution profile was monitored by A_{280}. Standards were run at the beginning and end of each data set to ensure that those proteins that flowed through the column without binding were not false negative results. Each experiment was performed in duplicate for all reported mutants.

The salt concentration corresponding to each eluted peak was calculated on the basis of the parameters described above and its position relative to the start of the gradient. Values are reported in millimolar NaCl and correspond to the center of the peak. An adjustment was made to account for the 60 mM NaCl offset caused by the 1.5 mL void volume between the mixing chamber and the detector.

Cellular Assays

Cell Cultures. CHO-K1 cells expressing apoaequorin and CCR5 were cultured using HAM's F12 medium supplemented with 10% fetal calf serum (Life Technologies), 100 units/mL penicillin, 100 mg/mL streptomycin (Life Technologies), 250 μg/mL zeocin (Invitrogen), and 400 mg/mL G418 (Life Technologies).

CCR5 Binding Assays. MIP-1β mutants were analyzed in competition binding experiments using a CCR5 CHO-K1 cell line and [^{125}I]MIP-1β as a tracer, as previously described (*18*). Briefly, 40 000 cells were incubated, for 90 min at 27 °C, with 0.08 nM [^{125}I]MIP-1β (2000 Ci/mmol, Amersham-Pharmacia) and variable concentrations of competitor. The bound tracer was separated by filtration through GF/B filters presoaked in 1% BSA. Filters were counted in a β-scintillation counter. Binding parameters were analyzed with PRISM software (GraphPad Software) using nonlinear regression applied to a one-site competition model. Competition binding with glycosidase-treated cells was performed as described above with cells (resuspended at a concentration of 4×10^6 cells/mL in binding buffer) that were preincubated with 1.0 IU/mL heparinase (EC 4.2.2.7, Sigma), 0.01 IU/mL heparinitase I (EC 4.2.2.8, Seikagaku), or 0.1 IU/mL chondroitinase ABC (EC 4.2.2.4, Seikagaku) or a combination of the three enzymes for 1 h at 37 °C. Competition binding experiments with soluble GAGs (heparin, heparan sulfate, chondroitin sulfate A, and chondroitin sulfate C) were performed as described above, and the results were analyzed by nonlinear regression applied to a one-site competition model using GraphPad PRISM software.

CCR5 Functional Assay. The functional response of CCR5 to the various MIP-1β mutants was analyzed by measuring the luminescence of aequorin as described previously (*18*). CHO-K1 cells coexpressing CCR5, apoaequorin, and $G_{\alpha 16}$ resuspended at a density of 5×10^6 cells/mL in DMEM/F12 were incubated in the dark for 4 h with 5 mM coelenterazine H (Molecular Probes). Before being used, the cells were diluted 5-fold, 50 mL of the cell suspension was added to 50 mL of medium containing the chemokines, and the luminescence was measured for 30 s in an EG&G-Berthold luminometer. Functional parameters were analyzed with GraphPad PRISM software using nonlinear regression applied to a sigmoidal dose−response model. The effect of heparinase, heparitinase I, and chondroitinase ABC treatment of cells on their functional response to MIP-1β was tested by preincubating the CCR5-expressing cells with the enzymes as described above. The effect of soluble GAGs on the functional response to different agonists was performed with the same functional assay. Different concentrations of GAGs were incubated with 10 nM MIP-1β, 100 nM MIP-1β-K45A/R46A/K48A, 100 nM CCK, 20 μM ATP, or 0.1% Triton X-100 in DMEM/F12 for 1 h at 4 °C. Then, 50 mL of a cell suspension was then added to 50 mL of the agonist/GAG mixture, and the luminescence was measured for 30 s in an EG&G-Berthold luminometer.

RESULTS

Several sets of mutants were produced to characterize the importance of the basic residues in MIP-1β function and to assess the possible effects of quaternary structure on the interaction between MIP-1β and heparin. Mutations were made to the basic residues in WT-MIP-1β, MIP-1β-P8A, and MIP(9), because of the differences observed in their quaternary structure under the conditions of our NMR studies, and also because of the activity differences of these proteins: wild-type MIP-1β is a stable dimer, P8A is fully monomeric in NMR studies yet retains near-WT activity and receptor binding ability, and MIP(9) is a monomer that can tightly bind but only weakly activate the CCR5 receptor (*19*).

Structural Characterization by NMR. Each of the analogues used in the functional assays was first observed by NMR to determine whether mutation had perturbed the structure of the protein. MIP-1β-K45A, MIP-1β-R46A, MIP-1β-K48A, and MIP-1β-K45A/R46A/K48A each retain the spectral attributes of WT-MIP-1β at pH 2.5, with little variation in peak positions other than for the peaks corresponding to the amides of the mutated residues (Figure 1 shows several representative spectra). While the proteins with single Ala replacements at pH 7 remained undetectable in NMR experiments due to protein aggregation, the triple mutant MIP-1β-K45A/R46A/K48A exhibited little or no such pH-dependent aggregation at pH 7, as demonstrated by the narrow lines in the HSQC, shown in Figure 1D. The protein is obviously folded at this pH, and the peaks associated with the N-terminal dimer interface are clearly present (Figure 1D), indicating that the structure of this MIP-1β variant at higher pH is consistent with that determined at pH 2.5.

Several charge mutations were made on top of the monomeric P8A variant of MIP-1β. These MIP-1β-P8A charge mutants retain many spectral features of the parent

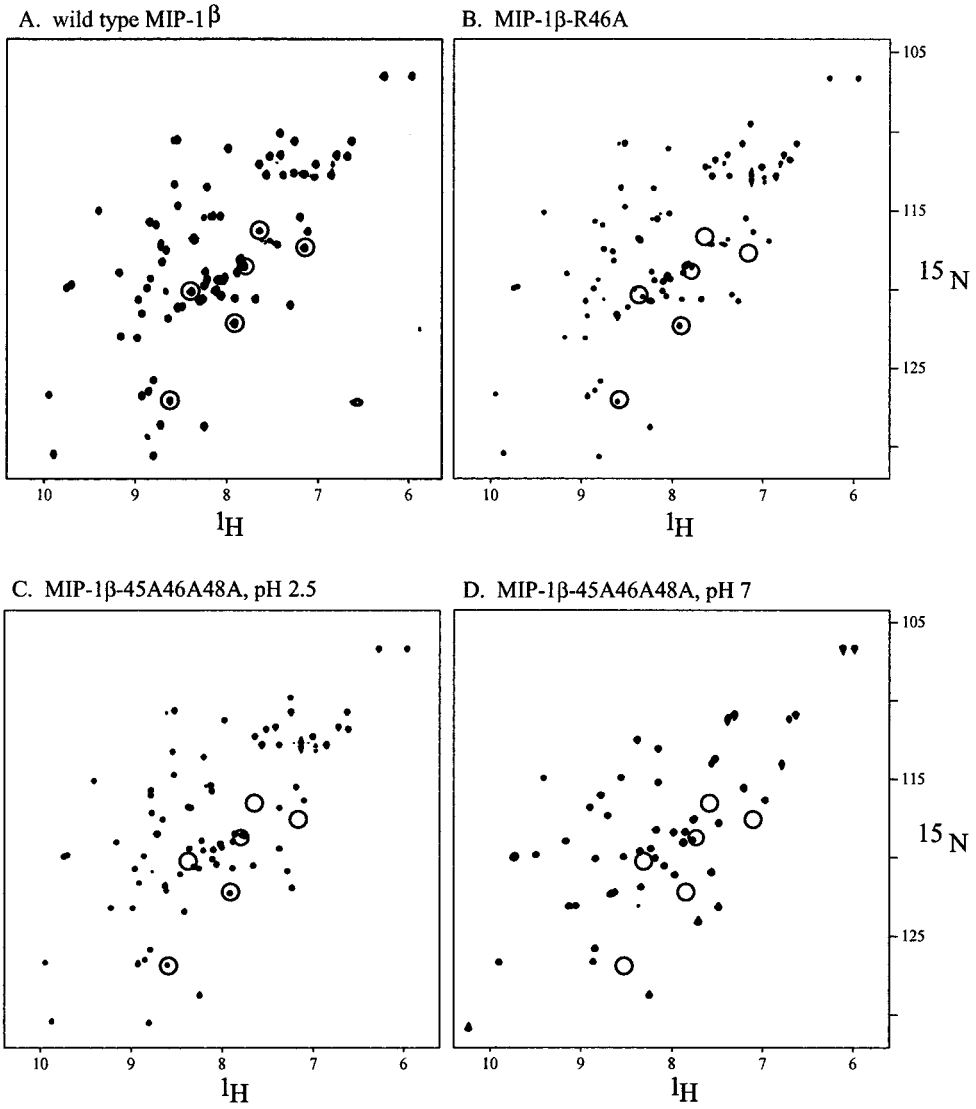

FIGURE 1: HSQC spectra of (A) WT-MIP-1β, (B) MIP-1β-R46A, and (C) MIP-1β-K45A/R46A/K48A in 20 mM sodium phosphate (pH 2.5) and (D) MIP-1β-K45A/R46A/K48A in 20 mM sodium phosphate (pH 7). Peaks enclosed in circles correspond to each of the basic residues in MIP-1β. Empty circles indicate that the mutation has resulted in a peak shift.

P8A monomer. However, additional peaks appear in the HSQC data of each analogue, due to the presence of 22 extraneous N-terminal amino acids resulting from incorrect proteolysis (data not shown).

Charge neutralization mutants were also constructed in the dimer-impaired truncation mutant MIP(9). The spectra of these analogues, having Ala substituted at each of the six positively charged amino acids, at pH 2.5 closely resemble that of MIP(9) and have minimal changes other than the peak corresponding to the mutated residue (except for the R22A variant which remained unfolded as described in Experimental Procedures; data not shown).

Heparin Binding. Heparin Sepharose chromatography is a well-established technique used to assess the ability of a protein to bind to physiological GAGs. Recently, it has been established that chemokine binding to a heparin sulfate column gives results analogous to those for chemokine binding to the cell surface sugar heparan sulfate (*11*) and to the sugars on human umbilical vein endothelial cells (*9*). WT-MIP-1β bound the heparin column and was eluted from it in 500 mM NaCl (Figure 2A and Table 1). As a control for non-specific anionic binding, MIP-1β was shown to not bind sp-sepharose at pH 6.1 (Pharmacia, data not shown). Basic residues in the 40's loop of MIP-1β were mutated individually, as well as simultaneously, to alanine. MIP-1β-K48A retained WT affinity for the column under the conditions that were tested, but the ability of R18A, K45A, and R46A to interact with heparin was modestly reduced, requiring 30, 60, and 80 mM lower salt concentrations for elution, respectively. Changing all three positively charged residues in the 40's loop to Ala (MIP-1β-K45A/R46A/K48A) destroyed the ability of the protein to bind heparin. The chromatographs for several of these proteins are shown in Figure 2.

To determine if heparin binding is concentration-dependent, MIP-1β-R46A was also diluted to $^1/_{10}$ the protein concentration and run over the heparin column. During this run, more than 50% of the protein flowed through the column without binding (data not shown). In addition, two peaks were eluted during the gradient in different proportions, in such a way that more protein eluted at lower ionic strength than when run at the higher protein concentration. The shift in elution does suggest that the strength of the interaction

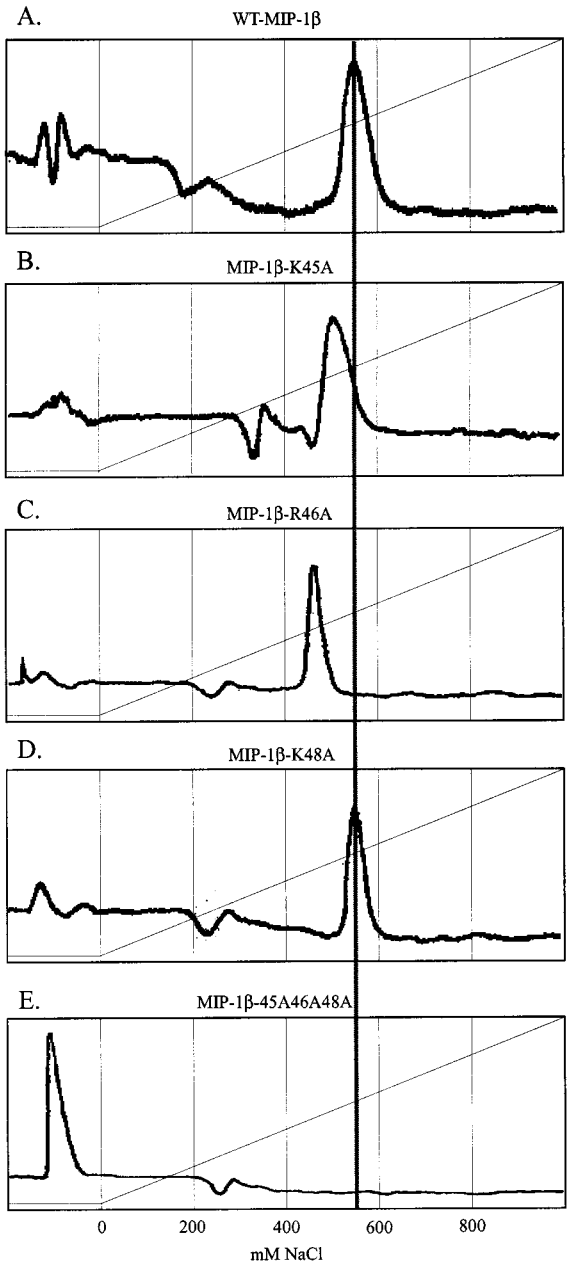

FIGURE 2: Heparin sulfate chromatography of wild type MIP-1β (A), MIP-1β-K45A (B), MIP-1β-R46A (C), MIP-1β-K48A (D), and MIP-1β-K45A/R46A/K48A (E). Proteins were loaded onto a 1 mL Hi-Trap heparin column and eluted with a 0 to 1 M NaCl gradient in 50 mM Tris (pH 7.4). A vertical line indicates the position at which WT-MIP-1β elutes.

between MIP-1β and heparin depends on the chemokine concentration.

The dimer-impaired truncation mutant MIP(9) bound heparin with wild-type affinity (500 mM NaCl), but a small percentage eluted early at 350 mM NaCl (Figure 3). Interestingly, the combination of the dimer-disabling MIP-(9) mutation with a charge mutation results in heparin binding changes that are much more dramatic than either type of mutation alone. For example, MIP(9)-R46A elutes at 260 nM NaCl, showing much weaker heparin binding than either MIP(9) or MIP-1β-R46A alone (Figure 3). More dramatically, although no loss of binding was observed for MIP-1β-K48A, adding this mutation to MIP(9) results in virtually complete abrogation of the protein−heparin interaction. Additionally, MIP-1β-K45A has an affinity for heparin near

Table 1: Average Salt Concentrations at Which Each Analogue of MIP-1β Elutes from a 1 mL Hi-Trap Heparin Sulfate Column[a]

protein	[NaCl] (mM)	difference from WT [NaCl] (mM)
WT-MIP-1β	500	0
MIP-1β-K45A	440	−60
MIP-1β-R46A	420	−80
MIP-1β-K48A	500	0
MIP-1β-K45A/R46A/K48A	NR	NR
MIP-1β-R18A	470	−30
MIP(9)	(350), 500	(−150), 0
MIP(9)-R18A	NR, 320, 480	NR, −180, −20
MIP(9)-K19A	320, 480	−180, −20
MIP(9)-K45A	NR	NR
MIP(9)-R46A	280	−220
MIP(9)-K48A	NR, (390)	NR, (−110)
MIP-1β-P8A	500	0
MIP-1β-P8A-mutants+tag	NR	NR
MIP-1β-F13A	NR, (310), 500	(−190), 0

[a] Multiple peaks were detected for several mutants. Peaks containing less than 10% of the total protein are shown in parentheses. For all proteins, there were no deviations between duplicate trials, except with WT and P8A, which were ±5 and 10 mM NaCl, respectively. The last column shows the difference in NaCl concentration between the WT elution and the mutants. Negative values represent a decrease in the level of binding compared to the wild-type protein. NR means no retention on column.

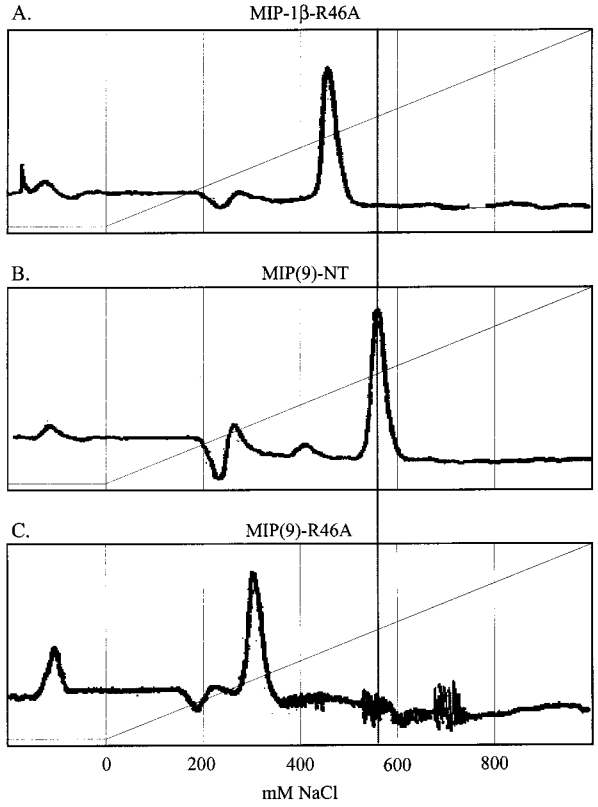

FIGURE 3: Elution profiles of MIP-1β-R46A (A), MIP(9) (B), and MIP(9)-R46A (C) run on a 1 mL heparin column in 50 mM Tris (pH 7.4) with a salt gradient of 0 to 1 M NaCl. A vertical line indicates the position at which WT-MIP-1β elutes.

that of WT, but the MIP(9)-K45A analogue fails to interact with heparin. MIP(9)-R18A and MIP(9)-K19A each have two peaks in their elution profiles corresponding to 300 and 460 mM NaCl, whereas the full-length MIP-1β-R18A mutant displays a single peak eluting at 470 mM NaCl (data not shown).

A different dimer-disabled variant, MIP-1β-P8A, also bound the heparin column with wild-type affinity. As described in Experimental Procedures, charge neutralization

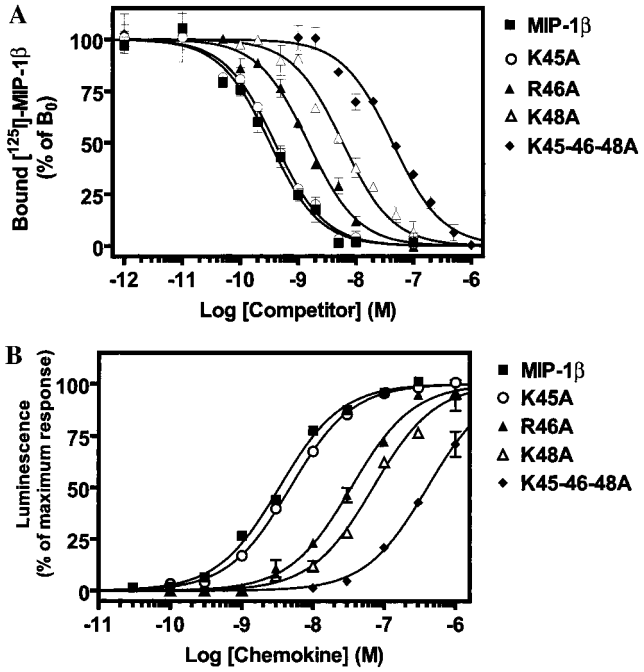

FIGURE 4: CCR5 activation and binding by MIP-1β analogues in which basic residues in the 40's loop have been mutated to alanine. (A) Competition binding curves were determined for CHO-K1 cell lines expressing CCR5 using 0.08 nM [^{125}I]MIP-1β as a tracer. Results were analyzed by GraphPad PRISM software, using a single-site model, and the data were normalized for nonspecific (0%) and specific binding in the absence of competitor (100%). All points were run in triplicate (error bars show the standard error of the mean). Data are representative of two independent experiments. (B) The functional response (luminescent signal recorded for 30 s) of the cell line coexpressing apoaequorin and CCR5 was tested following addition of MIP-1β mutants. Results were analyzed by nonlinear regression using GraphPad PRISM software. The data were normalized for basal (0%) and maximal luminescence (100%). All points were run in triplicate (error bars show the standard error of the mean). The displayed curves represent a typical experiment out of three performed independently.

mutants made in combination with the P8A mutation resulted in the presence of 22 amino acids at the N-terminus that were entirely resistant to cleavage by factor Xa. Every basic residue was replaced individually by Ala, and a triple mutation consisting of K45A, R46A, and K48A was introduced. All of these proteins were shown to be folded by NMR (although the extra amino acids were unstructured), but were completely incompetent at binding heparin and passed through the column unhindered.

MIP-1β mutant F13A, which has been shown to be a monomer and to exhibit a relative inability to bind CCR5 (*19*), was also analyzed for its ability to associate with heparin. About half of the loaded sample bound to heparin as well as the wild-type protein, eluting at 500 mM NaCl. However, early elution was observed at 310 mM NaCl for ~15% of the sample, and the other 35% eluted prior to the start of the gradient (data not shown).

Charge Mutants and CCR5 Function. Competition binding data were obtained for MIP-1β-K45A, MIP-1β-R46A, MIP-1β-K48A, and MIP-1β-K45A/R46A/K48A on CCR5 (Figure 4A and Table 2). Each of the mutants bound less tightly to the receptor than the WT protein, which had an IC_{50} of 410 pM. The IC_{50} for MIP-1β-K45A was 590 pM, and that of MIP-1β-R46A was 1.6 nM. The K48A mutation produced the largest loss in affinity of the three individual alanine

Table 2: Binding and Activation of CCR5 by MIP-1β Analogues[a]

protein	IC_{50} (nM)	EC_{50} (nM)
MIP-1β	0.41 ± 0.07	2.5 ± 0.7
MIP-1β-K45A	0.59 ± 0.20	4.0 ± 0.7
MIP-1β-R46A	1.55 ± 0.03	15.8 ± 5.8
MIP-1β-K48A	5.6 ± 0.4	33.9 ± 7.6
MIP-1β-K45A/R46A/K48A	31.6 ± 8.2	126 ± 43
MIP(9)	1.8 ± 0.3	43 ± 10
MIP(9)-R18A	1.7 ± 0.4	38 ± 12
MIP(9)-K19A	10 ± 3	145 ± 47
MIP(9)-K45A	49 ± 13	372 ± 137
MIP(9)-R46A	22 ± 6	182 ± 56
MIP(9)-K48A	27 ± 9	145 ± 47
MIP-1β-P8A	0.58 ± 0.09	11 ± 2
MIP-1β-P8A/K48A+tag	158 ± 49	537 ± 90

[a] Column 2 shows the IC_{50} value for each mutant obtained in a competitive binding assay with [^{125}I]MIP-1β. EC_{50} values, shown in column 3, correspond to the amount of protein at which 50% of the maximum activation of intracellular calcium stores is detected by a luminescence assay. The values are the mean ± the standard error of the mean resulting from at least three independent experiments.

replacement mutants with an IC_{50} of 5.6 nM. The affinity of the triple mutant for CCR5 was nearly 2 orders of magnitude lower than that of the wild-type protein, with an IC_{50} value of 32 nM. Calcium release assays were used to test the ability of the charge mutants to signal through CCR5 (Figure 4B and Table 2). MIP-1β-K45A produced a signal comparable to that of WT-MIP-1β (EC_{50} = 4 and 2.5 nM, respectively), but MIP-1β-R46A, MIP-1β-K48A, and MIP-1β-K45A/R46A/K48A exhibited large decreases in activity. The shift in EC_{50} for MIP-1β-R46A, MIP-1β-K48A, and MIP-1β-K45A/R46A/K48A (16, 34, and 126 nM, respectively) were approximately proportional to their decreases in receptor binding affinities.

The receptor binding affinity of the MIP(9) analogues for CCR5 was also determined (Table 2). The order of binding affinity is as follows: MIP(9) = MIP(9)-R18A > MIP(9)-K19A > MIP(9)-R46A > MIP(9)-K48A > MIP(9)-K45A. MIP(9) and MIP(9)-R18A have similar IC_{50} values of 1.8 and 1.7 nM, respectively, and MIP(9)-K19A exhibits a 5-fold decrease in comparison, with an IC_{50} of 10 nM. The R46A and K48A mutations resulted in an approximately 10-fold reduction in affinity compared to that of MIP(9) with IC_{50} values of 22 nM and 27 nM, respectively, whereas changing K45 to Ala produced the weakest binding affinity (IC_{50} = 49 nM). The trend in calcium signaling in these mutants is similar to that for binding (Table 2). As noted previously, MIP(9) acts as a partial agonist, displaying a weak ability to activate the CCR5 receptor as measured by the small amount of calcium released compared to the wild-type protein (*19*).

Each basic residue in MIP-1β-P8A was mutated to Ala as well. Due to the inability of the protease to remove the N-terminal tag correctly, only one mutant (MIP-1β-P8A/K48A+tag) was chosen for functional assay activity analysis. This protein bound and activated CCR5 quite poorly; full activation was not achieved at 1 μM, and the EC_{50} was estimated to be 540 nM (data not shown).

Effect of Cell Surface and Soluble GAGs on CCR5 Function. To determine the importance of cell surface glycosaminoglycans in the binding and functional response of CCR5 to MIP-1β, we investigated the effect of enzymatic removal of cell surface GAGs by glycosidases on the affinity of MIP-1β measured by homologous binding competition,

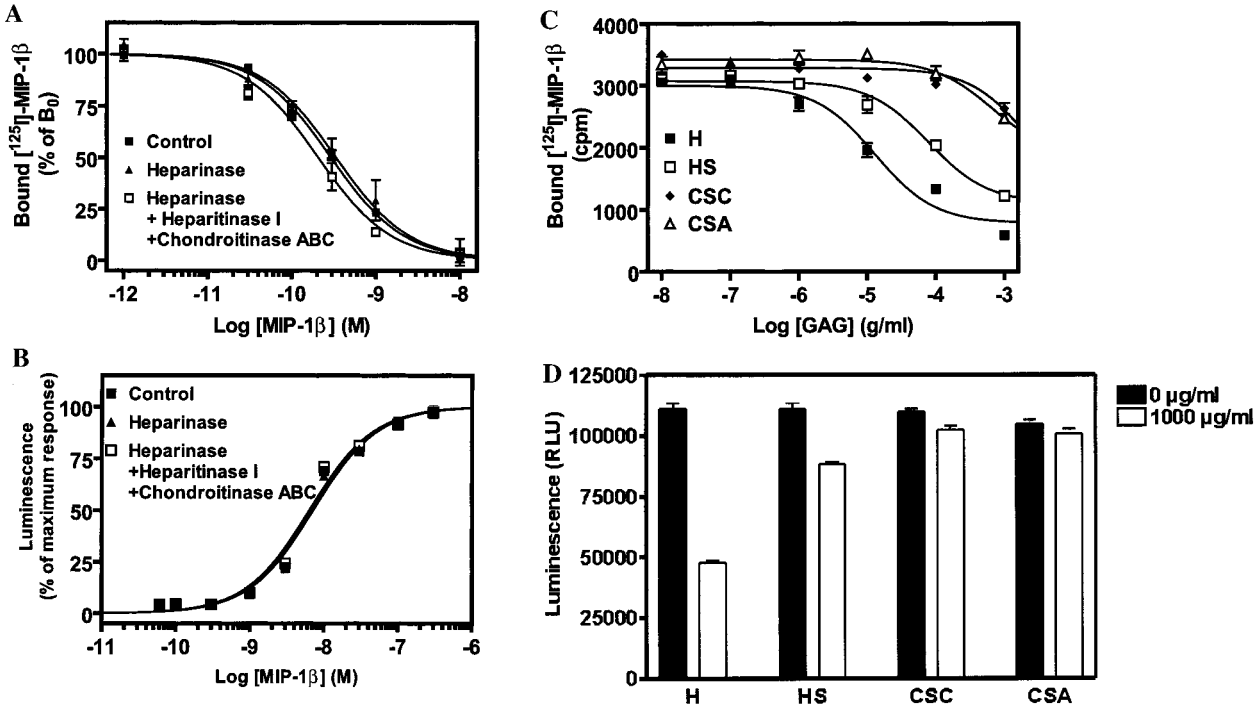

FIGURE 5: Effect of cell surface GAGs on MIP-1β binding to CCR5. (A) Binding of WT MIP-1β was assessed on CHO cells that had been treated with heparinase or a combination of heparinase, heparitinase I, and chondroitinase ABC. (B) The CCR5 activation by MIP-1β was assessed on CHO cells that had been treated with heparinase or a combination of heparinase, heparitinase I, and chondroitinase ABC. (C) Soluble GAGs and chemokine binding. The ability of several soluble GAGs to inhibit CCR5 binding by MIP-1β is shown: H, heparin; HS, heparan sulfate; CSC, chondroitin sulfate C; and CSA, chondroitin sulfate A. (D) Soluble GAGs and chemokine activity. The ability of several soluble GAGs to inhibit CCR5 activity by 10 nM MIP-1β is shown: H, heparin; HS, heparan sulfate; CSC, chondroitin sulfate C; and CSA, chondroitin sulfate A.

and on its ability to induce a functional response in CHO cells expressing CCR5. CHO-K1 cells express various GAGs that are able to bind chemokines. Bacterial polysaccharide lyases (heparinase, heparitinase I, and chondroitinase ABC) are enzymes with well-characterized specificities for GAGs. For example, cell surface heparan sulfate, assessed by FACS analysis using a specific monoclonal antibody, was totally removed from CHO cells by incubation with heparitinase I, whereas chondroitinase ABC had no effect (data not shown). Treatment of CCR5-expressing CHO cells with heparinase, heparitinase I, and chondroitinase ABC alone, or in combination, did not result either in a reduction of the ability of MIP-1β to compete for [^{125}I]MIP-1β binding (Figure 5A and data not shown) or in its ability to induce a functional response (Figure 5B and data not shown). Similarly, the abilities of MIP-1β mutants K45A and K45A/R46A/K48A to interact with CCR5 were essentially identical on normal cells and on cells treated to remove surface GAGs (data not shown). These results suggested that cell surface GAGs were not necessary for the high-affinity binding of MIP-1β to CCR5 or for the Ca^{2+} signaling resulting from this interaction.

The absence of a direct correlation between the affinities of MIP-1β mutants for heparin and for CCR5 but the reduction of binding affinity and functional response induced by the triple mutant MIP-1β-K45A/R46A/K48A led us to investigate whether the binding sites of MIP-1β for GAGs and for CCR5 were overlapping. One would expect that if the binding sites for GAG and CCR5 are spatially distinct, GAGs should not compete for the binding of MIP-1β to CCR5, although it is possible that GAGs may appear to compete but actually sequester MIP-1β without binding in the same location. We therefore investigated the effect of soluble GAGs on the binding of 0.08 nM [^{125}I]MIP-1β to CCR5.

As shown in Figure 5C, soluble GAGs inhibited the binding of [^{125}I]MIP-1β to CCR5 although with variable potency. Heparin was the most potent GAG inhibitor of [^{125}I]-MIP-1β binding to CCR5 with an IC_{50} of 16 $\pm$ 9 μg/mL, whereas the IC_{50} of heparan sulfate was about 10-fold higher (133 $\pm$ 48 μg/mL). Chondroitin sulfate C and A were much less potent with IC_{50} values of $>$1000 μg/mL.

We next investigated the importance of the competitive effect of soluble GAGs on the functional response induced by MIP-1β on the CHO cell line expressing CCR5. As shown in Figure 5D, more than 50% of the functional response induced by 10 nM MIP-1β was antagonized by 1000 μg/mL heparin. As for competition binding experiments, heparan sulfate was less potent than heparin, inhibiting less than 25% of the functional response to MIP-1β at 1000 μg/mL, whereas chondroitin sulfates did not inhibit the functional response at the highest concentration that was tested. To test whether the inhibitory effect of soluble GAGs on MIP-1β-induced signaling was secondary to the formation of a GAG$-$MIP-1β complex, we tested the effect of soluble GAGs on the functional response induced by the mutant MIP-1β-K45A/R46A/K48A that could no longer bind heparin or by various agents that promote intracellular calcium signaling in CHO cells. Addition of soluble GAGs had no effect on the response mediated by 10 nM MIP-1β-K45A/R46A/K48A, 100 nM CCK, 10 μM ATP, or 0.1% Triton X-100, demonstrating that this inhibitory effect is linked to the ability of GAG to bind MIP-1β (Figure 5D and data not shown).

DISCUSSION

Different chemokines have been shown to require basic residues located in various regions of the protein to bind GAGs. MCP-1 and PF-4 contain residues in their C-terminal α-helix that participate in GAG binding (*13*, *42*), whereas basic residues along the β1 strand of SDF-1 have been shown to be important for interaction (*43*). Mutation of basic amino acids in MIP-1α reveals that the residues involved in GAG binding are located in two loops (*10*,*12*). Comparison of the protein sequences for the CC chemokine subfamily reveals that the basic residues at positions 18, 45, 46, and 48 are well conserved, while basic amino acids at other positions vary. Our data show that the conserved basic residues in MIP-1β are involved in heparin binding, with those located in the 40's loop having particular importance. Koopmann et al. recently characterized the heparin binding properties of MIP-1β (*11*) and established that retention on a heparin column provides an accurate assessment of the ability of MIP-1β to bind to the cell surface sugar heparan sulfate. These workers replaced each positively charged residue in MIP-1β with alanine, and concluded that R46 was necessary for GAG binding, R18 and K45 were of minor importance, and the other three positive charges (K19, R22, and K48) were unimportant for GAG binding (*11*). Using an overlapping set of mutants, we reached somewhat different conclusions (Table 1).

The disparity in heparin binding results for the R46A mutant between our lab and that of Koopmann et al. can be explained by the significant difference in the protein concentrations that were used (*11*); i.e., Koopmann's experiments were carried out at a lower chemokine concentration than were ours. Although our experiments show that MIP-1β-R46A bound rather well at high protein concentrations, we observed a decrease in this mutant's ability to interact with heparin when diluted 10-fold. The result of this intermediate concentration suggests that R46 does contribute to heparin binding. The dependence on protein concentration of affinity for the GAG indicates that the lower concentrations may be near the GAG−MIP-1β dissociation constant, and also suggests the possibility that formation of a MIP-1β−heparin complex requires self-association of the chemokine.

Physiologically, chemokines form concentration gradients that recruit lymphocytes to infected or injured regions, and these gradients are believed to be stabilized by the interaction of chemokines with GAGs from the cell surface and the extracellular matrix. Since GAGs have been shown to mediate multimerization of several chemokines, including RANTES, MIP-1α, and MCP-1 (*7*), it has been suggested that the quaternary state of the chemokine may play a role in the ability to bind GAGs (*11*, *19*, *24*), and as such, protein concentration may indeed play a role in the ability of the chemokine variants to bind heparin. The role of chemokine multimerization in GAG binding is further complicated by the charge-mediated aggregation undergone by MIP-1β, MIP-1α, and RANTES. Czaplewski et al. (*44*) have shown that mutation of certain negatively charged residues reduces the ability of these chemokines to self-aggregate. In addition, we show by NMR that when the 40's loop of MIP-1β is completely neutralized (K45A/R46A/K48A) the protein does not undergo pH-dependent aggregation and it loses the ability to bind heparin. Therefore, the charge mutants of Koopmann et al. may exhibit a larger reduction in their ability to bind heparin due to an inability to multimerize both because of lower concentrations and because certain charges may help to assemble the correct chemokine quaternary structure. Therefore, the combination of the data presented here with that previously reported indicates that the 40's loop of MIP-1β is critical to GAG binding, with R46 being the single most important residue.

Comparison of Monomers and Dimers. MIP-1β self-associates by two different mechanisms. First, the dimer interface of the chemokine is hydrophobic in nature and involves the N-terminus of the protein. Mutations aimed at removing key hydrophobic interactions result in the loss of the ability to form a dimer under the low-pH conditions generally used for study of this protein (*19*). Second, self-association above the level of dimer occurs in a pH-dependent fashion and is mediated by charge interactions (*44*). An intact dimer may not be necessary for pH-mediated aggregation, as three different monomeric MIP-1β variants [MIP(9), MIP-1β-P8A, and MIP-1β-F13A] retain the ability to aggregate as evidenced by the loss of the NMR signal at pH $>$3.5 (data not shown). It is possible, however, that the charge interactions involved in this multimerization also promote the formation of the usual dimer interface even in these "monomeric" variants. As it has been postulated that the dimer form of chemokines is utilized in GAG binding (*11*, *19*, *24*), we undertook a comparison of the heparin binding ability of MIP-1β and its dimer-impaired variants.

MIP(9), MIP-1β-P8A, and MIP-1β-F13A were all shown to have diminished capacities for dimerization, but each remains largely capable of binding heparin as well as the wild-type protein (Table 1). However, the presence of multiple peaks in the elution profiles for these mutants (as compared to one clean peak for the wild-type protein) suggests that more than one conformation or quaternary state may be binding to the heparin.

Interestingly, when the dimer-impaired MIP(9) is further mutated to neutralize any of the charged amino acids in the 40's loop, the protein behaves dramatically differently from the analogous charge-neutralized full-length protein (Table 1). For example, while the K45A and K48A mutations in MIP-1β result in little change in the ability of the protein to bind heparin, when these mutations are made to the truncated MIP(9) variant, the protein becomes essentially unable to bind heparin. The effects are similar, although not as dramatic, for other charge mutations on top of the MIP(9) monomer, including R18A, K19A, and R46A. This obvious disparity in heparin binding affinities of full-length MIP-1β containing charge neutralization and the truncated MIP(9) analogues possessing the same mutations was surprising since MIP(9) itself binds heparin with seemingly the same affinity as the WT. Since the major difference between the two sets of mutants is the ability to form a dimer, the data suggest that the ability of MIP-1β to dimerize is involved in binding GAGs. An interesting question arising from these experiments is why the R46A mutation on top of MIP(9) does not produce as dramatic a loss of GAG binding as other mutations, when R46A is an important mediator of the MIP-1β−GAG interaction. One possible explanation is that there are subtle differences in structure in the 40's loop region between the dimeric and monomeric form of MIP-1β.

In general, monomeric variants of MIP-1β have different elution profiles than dimeric variants, often having a portion of the protein elute early in the gradient (Table 1). These multiple peaks on the chromatogram suggest that the protein may consist of multiple conformational states and that quaternary structure may play a role in heparin affinity. It is possible that MIP-1β interacts with GAGs in more than one quaternary state, particularly since this chemokine is known to undergo aggregation under a variety of conditions. More extensive analysis of this chemokine will be undertaken at various concentrations to elucidate the specific details of how quaternary structure participates in the formation of a chemokine−GAG complex.

Residues in the 40's Loop Are Involved in CCR5 Binding. Full-length MIP-1β proteins mutated at positions 46 and 48 exhibited reduced abilities to bind CCR5 compared to the wild-type protein. The K48A mutant showed the most dramatic loss of receptor binding ability among the single mutants, and the triple mutant MIP-1β-K45A/R46A/K48A showed poor binding (Figure 4A) despite being completely folded as shown by NMR (Figure 1). This work delineates a new 40's loop receptor binding surface on MIP-1β, as prior experiments have shown that residue 13 in the N-loop region (residues 13−20) is important for receptor binding (*19*) and those at the N-terminus are involved in signaling (*14*−*19*). Basic residues outside the N-loop region have also been shown to be important in receptor binding by the chemokine MCP-1 (*45*). Examination of the NMR structures of CC chemokines shows that the 40's loop residues are relatively distant from the N-loop on the monomeric subunit. Although on approximately the same side of the protein surface, the N-loop in combination with the 40's loop spans a distance of approximately 25 Å. The side chain of Phe13, a residue in the N-loop shown to be crucial for CCR5 binding (*19*), and the ϵ-amino group of Lys48 in MIP-1β are nearest to each other at 15 Å. It is more difficult to predict distances with N-terminal residues since the N-terminal region is not well structured in the chemokine monomer. Nonetheless, in the published structure of MIP-1β, the N-terminus is as much as 40 Å away from the positive charges in the 40's loop of the same subunit (*26*), suggesting that the receptor−chemokine interaction may involve much of the chemokine's surface area. Although previous work has shown that monomers can interact with CCR5 (*19*), it is interesting that despite the large distances between the 40's loop and the N-terminus in the monomer, in the dimer the N-terminus of one subunit is in proximity to the 40's loop of the second subunit, in such a way that Pro2 is within 3.3 Å of Arg46′.

Despite the clear decrease in CCR5 binding affinities for the MIP-1β analogues mutated in the 40's loop, no direct correlation can be made between the ability of these residues to affect heparin binding and their association with CCR5. K48A bound heparin as well as WT MIP-1β in our assay, yet displayed the weakest affinity for CCR5. Approximately equivalent reductions in heparin binding ability were observed for K45A and K48A, but their abilities to bind the receptor were nearly 1 order of magnitude different from each other, with K45A binding almost as well to CCR5 as WT MIP-1β. Therefore, it appears that several residues in MIP-1β are important for both receptor binding and GAG binding, in such a way that some of the same amino acids are involved in each action but not to a parallel extent.

The results from the calcium flux assays show that EC_{50} of MIP-1β mutants is proportional to IC_{50} measured in binding assays. Therefore, we can conclude that K45, R46, and K48 in MIP-1β are not involved in receptor activation, but are principally involved in receptor binding. The results reported by Czaplewski et al. (*44*) showing that mutation of these residues in the related protein MIP-1α reduced their biological activity may likely be due to reduced receptor binding. While Koopmann et al. carried out a chemotaxis assay on one MIP-1β variant (R46A) and concluded that this variant has the same activity as the wild-type protein (*11*), the work presented here represents a full functional comparison of a family of MIP-1β variants, having differing abilities to bind heparin, and shows that the 40's loop is a receptor binding determinant of MIP-1β.

Influence of Cell Surface and Soluble GAGs on CCR5 Binding. Although there is general agreement that the ability of chemokines to bind GAGs has functional relevance, the precise nature of the effect of GAGs on chemokine activity is not clear, particularly with respect to receptor binding. The presence of GAGs has been demonstrated to be important to the anti-HIV activity of RANTES and MIP-1β (*37*, *38*, *46*). An interpretation of these results might suggest a direct link between the ability of a chemokine to bind cell surface GAGs and its ability to bind CCR5 to lock out HIV. In support of this, it has been reported that the addition of soluble GAGs enhances the anti-HIV activity of RANTES (*38*). However, in contrast to this interpretation, when direct investigations of receptor binding were carried out, it was shown that soluble GAGs compete with the receptor for chemokine binding and block the ability of RANTES and MIP-1α to interact with both CCR1 and CCR5 (*9*, *39*). Further, in cells genetically altered to eliminate expression of cell surface sugars, receptor binding by RANTES and MIP-1β was shown to be largely unchanged (*39*). Our results concur with these, showing that the ability of MIP-1β to bind CCR5 is insensitive to the presence of GAGs at the cell surface. No decrease in the ability to bind and activate CCR5 was observed in response to WT-MIP-1β after surface GAGs were removed. Furthermore, addition of soluble GAGs (heparin, heparan sulfate, and chondroitin sulfates) inhibited MIP-1β binding to CCR5 and Ca^{2+} signaling, although with variable potency. MIP-1β was much more affected by the heparin, heparan sulfate GAGs subfamily than chondroitin sufates. The effect of membrane and soluble GAGs on HIV infection may therefore be the result of several interactions and not simply a reflection of the chemokine's ability to bind CCR5 and block HIV entry.

CONCLUSION

We have investigated the contribution of basic residues to the function of the chemokine MIP-1β and to the ability of MIP-1β to bind to glycosaminoglycans. GAGs may provide the mechanism by which particular cells sequester the appropriate chemokines on their surfaces to allow chemotaxis and receptor activation. The basic residues in the 40's loop of MIP-1β (K45, R46, and K48) have been shown to be important in receptor binding and also in GAG binding, although there is not a direct correlation between a residue's extent of involvement in receptor binding and its ability to mediate GAG binding. It appears that the ability to dimerize strengthens the association between MIP-1β and

heparin, as dimer-impaired mutants with a mutation to any of the basic residues are much less able to bind heparin than the full-length form of MIP-1β containing the same mutation. There is a clear indication that GAGs at the cell surface do not affect the ability of MIP-1β to interact with CCR5 or to promote intracellular calcium release, as enzymatic digestion of these sugars does not impair MIP-1β function.

ACKNOWLEDGMENT

We appreciate the technical assistance of Shu-chuan Jao. The NMR instrumentation in the Biomolecular NMR Laboratory at Texas A&M University was supported by a grant from the National Science Foundation (DBI-9970232) and the Texas A&M University System.

REFERENCES

1. Gilat, D., Hershkoviz, R., Mekori, Y. A., Vlodavsky, I., and Lider, O. (1994) *J. Immunol. 153*, 4899−4906.
2. Pantoliano, M. W., Horlick, R. A., Springer, B. A., Van Dyk, D. E., Tobery, T., Wetmore, D. R., Lear, J. D., Nahapetian, A. T., Bradley, J. D., and Sisk, W. P. (1994) *Biochemistry 33*, 10229−10248.
3. Spivak-Kroizman, T., Lemmon, M. A., Dikic, I., Ladbury, J. E., Pinchasi, D., Huang, J., Jaye, M., Crumley, G., Schlessinger, J., and Lax, I. (1994) *Cell 79*, 1015−1024.
4. Ornitz, D. M., Yayon, A., Flanagan, J. G., Svahn, C. M., Levi, E., and Leder, P. (1992) *Mol. Cell. Biol. 12*, 240−247.
5. Faham, S., Hileman, R. E., Fromm, J. R., Linhardt, R. J., and Rees, D. C. (1996) *Science 271*, 1116−1120.
6. Ogura, K., Nagata, K., Hatanaka, H., Habuchi, H., Kimata, K., Tate, S., Ravera, M. W., Schlessinger, J. M., and Inagaki, F. (1999) *J. Biomol. NMR 13*, 11−24.
7. Hoogewerf, A. J., Kuschert, G. S. V., Proudfoot, A. E. I., Borlat, F., Clark-Lewis, I., Power, C. A., and Wells, T. N. C. (1997) *Biochemistry 36*, 13570−13578.
8. Kuschert, G. S. V., Hoogewerf, A. J., Proudfoot, A. E. I., Chung, C., Cooke, R. M., Hubbard, R. E., Wells, T. N. C., and Sanderson, P. N. (1998) *Biochemistry 37*, 11193−11201.
9. Kuschert, G. S., Coulin, F., Power, C. A., Proudfoot, A. E., Hubbard, R. E., Hoogewerf, A. J., and Wells, T. N. (1999) *Biochemistry 38*, 12959−12968.
10. Koopmann, W., and Krangel, M. S. (1997) *J. Biol. Chem. 272*, 10103−10109.
11. Koopmann, W., Ediriwickrema, C., and Krangel, M. S. (1999) *J. Immunol. 163*, 2120−2127.
12. Graham, G. J., Wilkinson, P. C., Nibbs, R. J. B., Lowe, S., Kolset, S. O., Parker, A., Freshney, M. G., Tsang, M. L.-S., and Pragnell, I. B. (1996) *EMBO J. 15*, 6506−6515.
13. Chakravarty, L., Rogers, L., Quach, T., Breckenridge, S., and Kolattukudy, P. E. (1998) *J. Biol. Chem. 273*, 29641−29647.
14. Clark-Lewis, I., Kim, K.-S., Rajarathnam, K., Gong, J.-H., Dewald, B., Moser, B., Baggiolini, M., and Sykes, B. D. (1995) *J. Leukocyte Biol. 57*, 703−711.
15. Gong, J.-H., and Clark-Lewis, I. (1995) *J. Exp. Med. 181*, 631−640.
16. Gong, J.-H., Uguccioni, M., Dewald, B., Baggiolini, M., and Clark-Lewis, I. (1996) *J. Biol. Chem. 271*, 10521−10527.
17. Pakianathan, D. R., Kuta, E. G., Artis, D. R., Skelton, N. J., and Hebert, C. A. (1997) *Biochemistry 36*, 9642−9648.
18. Weber, M., Uguccioni, M., Baggiolini, M., Clark-Lewis, I., and Dahinden, C. A. (1996) *J. Exp. Med. 183*, 681−685.
19. Laurence, J. S., Blanpain, C., Burgner, J. W., Parmentier, M., and LiWang, P. J. (2000) *Biochemistry 39*, 3401−3409.
20. LiWang, A. C., Cao, J. J., Zheng, H., Lu, Z., Peiper, S. C., and LiWang, P. J. (1999) *Biochemistry 38*, 442−453.
21. Sticht, H., Escher, S. E., Schweimer, K., Forssmann, W.-G., Rosch, P., and Adermann, K. (1999) *Biochemistry 38*, 5995−6002.
22. Mayer, K. L., and Stone, M. S. (2000) *Biochemistry 39*, 8382−8395.
23. Keizer, D. W., Crump, M. P., Lee, T. W., Slupsky, C. M., Clark-Lewis, I., and Sykes, B. D. (2000) *Biochemistry 39*, 6053−6059.
24. Paavola, C. D., Hemmerich, S., Grunberger, D., Polsky, I., Bloom, A., Freedman, R., Mulkins, M., Bhakta, S., McCarley, D., Wiesent, L., Wong, B., Jarnagin, K., and Handel, T. M. (1998) *J. Biol. Chem. 273*, 33157−33165.
25. Rajarathnam, K., Kay, C. M., Dewald, B., Wolf, M., Baggiolini, M., Clark-Lewis, I., and Sykes, B. D. (1997) *J. Biol. Chem. 272*, 1725−1729.
26. Lodi, P. J., Garrett, D. S., Kuszewski, J., Tsang, M. L., Weatherbee, J. A., Leonard, W. J., Gronenborn, A. M., and Clore, G. M. (1994) *Science 263*, 1762−1767.
27. Clore, G. M., Appella, E., Yamada, M., Matsushima, K., and Gronenborn, A. M. (1990) *Biochemistry 29*, 1689−1696.
28. Skelton, N. J., Aspiras, F., Ogez, J., and Schall, T. J. (1995) *Biochemistry 34*, 5329−5342.
29. Meunier, A., Bernassau, J.-M., Guillemot, J.-C., Ferrara, P., and Darbon, H. (1997) *Biochemistry 36*, 4412−4422.
30. Handel, T. M., and Domaille, P. J. (1996) *Biochemistry 35*, 6569−6584.
31. Lubkowski, J., Bujacz, G., Boque, L., Domaille, P. J., Handel, T. M., and Wlodawer, A. (1997) *Nat. Struct. Biol. 4*, 64−69.
32. Rajarathnam, K., Sykes, B. D., Kay, C. M., Dewald, B., Geiser, T., Baggiolini, M., and Clark-Lewis, I. (1994) *Science 264*, 90−92.
33. Deng, H., Liu, R., Ellmeier, W., Choe, S., Unutmaz, D., Burkhart, M., Di Marzio, P., Marmon, S., Sutton, R. E., Hill, C. M., Davis, C. B., Peiper, S. C., Schall, T. J., Littman, D. R., and Landau, N. R. (1996) *Nature 381*, 661.
34. Alkhatib, G., Combadiere, C., Broder, C. C., Feng, Y., Kennedy, P. E., Murphy, P. M., and Berger, E. A. (1996) *Science 272*, 1955−1958.
35. Drajic, T., Litwin, V., Allaway, G. P., Martin, S. R., Huang, Y., Nagashima, K. A., Cayanan, C., Maddon, P. J., Koup, R. A., Moore, J. P., and Paxton, W. A. (1996) *Nature 381*, 667−673.
36. Samson, M., Labbe, O., Mollereau, C., Vassart, G., and Parmentier, M. (1996) *J. Biol. Chem. 35*, 3362−3367.
37. Oravecz, T., Pall, M., Wang, J., Roderiquez, G., Ditto, M., and Norcross, M. A. (1997) *J. Immunol. 159*, 4587−4592.
38. Wagner, L., Yang, O. O., Garcia-Zepeda, E. A., Ge, Y., Kalams, S. A., Walker, B. D., Pasternack, M. S., and Luster, A. D. (1998) *Nature 391*, 908−911.
39. Ali, S., Palmer, A. C. V., Banerjee, B., Fritchley, S. J., and Kirby, J. A. (2000) *J. Biol. Chem. 275*, 11721−11727.
40. Wishart, D. S., Bigam, C. G., Yao, J., Abildgaard, F., Dyson, H. J., Oldfield, E., Markley, J. L., and Sykes, B. D. (1995) *J. Biomol. NMR 6*, 135−140.
41. Delaglio, F., Gresiek, S., Vuister, G. W., Zhu, G., Pfeifer, J., and Bax, A. (1995) *J. Biomol. NMR 6*, 277−293.
42. Stuckey, J. A., St Charles, R., and Edwards, B. F. (1992) *Proteins 14*, 277−287.
43. Amara, A., Lorthioir, O., Valenzuela, A., Magerus, A., Thelen, M., Montes, M., Virelizier, J. L., Delepierre, M., Baleux, F., Lortat-Jacob, H., and Arenzana-Seisdedos, F. (1999) *J. Biol. Chem. 274*, 23916−23925.
44. Czaplewski, L. G., McKeating, J., Craven, C. J., Higgins, L. D., Appay, V., Brown, A., Dudgeon, T., Howard, L. A., Meyers, T., Owen, J., Palan, S. R., Tan, P., Wilson, G., Woods, N. R., Heyworth, C. M., Lord, B. I., Brotherton, D., Christison, R., Craig, S., Cribbes, S., Edwards, R. M., Evans, S. J., Gilbert, R., Morgan, P., Hunter, M. G., et al. (1999) *J. Biol. Chem. 274*, 16077−16084.
45. Hemmerich, S., Paavola, C., Bloom, A., Bhakta, S., Freedman, R., Grunberger, D., Krstenansky, J., Lee, S., McCarley, D., Mulkins, M., Wong, B., Pease, J., Mizoue, L., Mirzadegan, T., Polsky, I., Thompson, K., Handel, T. M., and Jarnagin, K. (1999) *Biochemistry 38*, 13013−13025.
46. Burns, J. M., Lewis, G. K., and DeVico, A. L. (1999) *Proc. Natl. Acad. Sci. U.S.A. 96*, 14499−14504.

BI002593W